

KINETIC STUDY AND CHARACTERIZATION OF BORIDED AISI 4140 STEEL

ŠTUDIJA KINETIKE IN KARAKTERIZACIJA BORIRANEGA JEKLA AISI 4140

**Mourad Keddami¹, Martín Ortiz-Domínguez², Oscar Armando Gómez-Vargas³,
Alberto Arenas-Flores⁴, Miguel Ángel Flores-Rentería², Milton Elias-Espinosa⁵,
Abel García-Barrientos⁶**

¹Département de Sciences des Matériaux, Faculté de Génie Mécanique et Génie des Procédés, USTHB, B.P. No. 32, 16111 El-Alia, Bab-Ezzouar, Algiers, Algeria

²Universidad Autónoma del Estado de Hidalgo, Escuela Superior de Ciudad Sahagún-Ingeniería Mecánica, Carretera Cd. Sahagún-Otumba s/n, Zona Industrial CP. 43990 Hidalgo, México

³Instituto Tecnológico de Tlalnepantla-ITTLA. Av., Instituto Tecnológico, S/N. Col. La Comunidad, Tlalnepantla de Baz. CP. 54070 Estado de México, México

⁴Universidad Autónoma del Estado de Hidalgo-AACTyM, Carretera Pachuca Tulancingo Km. 4.5, Mineral de la Reforma, CP. 42184 Hidalgo, México

⁵Instituto Tecnológico y de Estudios Superiores de Monterrey-ITESM Campus Santa Fe, Av. Carlos Lazo No. 100, Del. Álvaro Obregón, CP. 01389 D. F., México

⁶Universidad Autónoma del Estado de Hidalgo-CITIS, Carretera Pachuca Tulancingo Km. 4.5, Mineral de la Reforma, CP. 42184 Hidalgo, México
keddami@yahoo.fr

Prejem rokopisa – received: 2014-02-11; sprejem za objavo – accepted for publication: 2014-10-08

doi:10.17222/mit.2014.034

In the present study, an alternative diffusion model was proposed for analyzing the growth of Fe₂B layers formed on the AISI 4140 steel during the pack-boriding process. This model was based on solving the mass-balance equations for the Fe₂B/Fe interface to evaluate boron diffusion coefficients through the Fe₂B layers in a temperature range of 1123–1273 K. The boride incubation time for the Fe₂B phase was included in the present model. The suggested model was validated experimentally at a temperature of 1253 K for a treatment time of 5 h. Furthermore, the generated boride layers were analyzed with light microscopy, scanning electron microscopy (SEM), energy dispersive X-ray spectroscopy (EDS) and X-ray diffraction analysis (XRD). In addition, a contour diagram was also proposed as a function of treatment time and temperature. On the basis of our experimental results, the boron activation energy for the AISI 4140 steel was found to be 189.24 kJ mol⁻¹.

Keywords: boriding, incubation time, diffusion model, growth kinetics, activation energy, adherence

V tej študiji je predlagan alternativni model difuzije za analiziranje rasti Fe₂B-plasti, ki nastane na jeklu AISI 4140 pri boriranju v škatli. Ta model temelji na rešitvi enačbe ravnotežja mas na stiku (Fe₂B/Fe) pri oceni koeficienta difuzije bora skozi Fe₂B-sloje v temperaturnem območju 1123–1273 K. Inkubacijski čas borida za Fe₂B-fazo je bil vključen v predstavljeni model. Predlagani model je bil eksperimentalno ocenjen pri temperaturi 1253 K in času obdelave 5 h. Poleg tega so bili izdelani sloji analizirani na svetlobnem mikroskopu, z vrstičnim elektronskim mikroskopom (SEM), energijsko disperzijsko rentgensko spektroskopijo (EDS) in z rentgensko difrakcijsko analizo (XRD). Dodatno je bil predlagan še konturni diagram kot funkcija časa obdelave in temperature. Na podlagi eksperimentalnih rezultatov je bilo ugotovljeno, da je aktivacijska energija bora pri jeklu AISI 4140 189,24 kJ mol⁻¹.

Gljučne besede: boriranje, čas inkubacije, model difuzije, kinetika rasti, aktivacijska energija, aderenza

1 INTRODUCTION

Boriding is a well-known thermochemical treatment in which boron (because of its relatively small size) diffuses into the metal substrate to form hard borides. As a result of boriding, properties such as wear resistance, surface hardness and corrosion resistance are improved.¹ Boriding can be carried out with boron in different states such as solid powder, paste, liquid, gas and plasma. The most frequently used method is pack boriding owing to its technical advantages.² Generally, the commercial boriding mixture is composed of boron carbide (B₄C) as a donor, KBF₄ as an activator and silicon carbide (SiC) as a diluent to control the boriding potential of the medium. The boriding treatment requires temperatures ranging

from 800 °C to 1000 °C. Usually the treatment time varies between 0.5 h and 12 h producing a boride layer whose thickness depends on the boriding parameters (time and temperature). The morphology of the boride layer is affected by the presence of alloying elements in the matrix. Saw-tooth-shaped layers are obtained in low-alloy steels or Armco iron whereas in high-alloy steels, the interfaces are smooth. According to the Fe-B phase diagram,³ two iron borides can be formed (FeB and Fe₂B).

A monophase Fe₂B layer with a tooth-shaped morphology is generally suitable for industrial applications because of the difference between the specific volume and the coefficients of the thermal expansion of iron

boride and the substrate.^{4,5} The boron-rich phase FeB is not preferred since FeB is more brittle and less tough than Fe₂B.^{4,5} Furthermore, the brittleness of FeB layers causes a spalling when a high normal or tangential load is applied.

The modeling of the boriding kinetics is considered as a suitable tool to select the optimized parameters for obtaining a desired boride layer of the treated material for its practical use in the industry. In particular, many models reported in the literature were used for analyzing the kinetics of the Fe₂B layers grown on different substrates⁶⁻¹⁶, with and without the boride incubation times.

In the current work, an alternative diffusion model, based on solving the mass-balance equation for the Fe₂B/substrate interface, was proposed to simulate the kinetics of the Fe₂B layers grown on the AISI 4140 steel. In the present model, the boride incubation time was independent of the temperature. The pack-borided AISI 4140 steel was characterized by means of the following techniques: light microscopy, scanning electron microscopy and XRD. Based on the experimental data, the boron activation energy was also evaluated when pack boriding the AISI 4140 steel in a temperature range of 1123–1273 K.

2 KINETIC MODEL

The model considers the growth of the Fe₂B layer on a substrate saturated with boron atoms as illustrated in **Figure 1**. The $f(x,t)$ function represents the boron distribution in the iron matrix before the nucleation of the Fe₂B phase. $t_0^{Fe_2B}$ corresponds to the incubation time required to form the Fe₂B phase when the matrix reaches the state of being saturated with boron atoms. $C_{up}^{Fe_2B}$ represents the upper limit of the boron content in Fe₂B ($60 \cdot 10^3 \text{ mol m}^{-3}$), $C_{low}^{Fe_2B}$ is the lower limit of the boron content in Fe₂B ($59.8 \cdot 10^3 \text{ mol m}^{-3}$) and the point $x(t=t)$ = v represents the Fe₂B layer thickness.^{17,18}

The term C_{ads}^B represents the effective adsorbed boron concentration during the boriding process.¹⁹ In **Figure 1**, $a_1 = C_{up}^{Fe_2B} - C_{low}^{Fe_2B}$ defines the homogeneity range of the Fe₂B layer, $a_2 = C_{low}^{Fe_2B} - C_0$ is the miscibility gap^{15,16} and C_0 is the boron solubility in the matrix considered as zero.³ The following assumptions are considered for the diffusion model:

- The growth kinetics is controlled by the boron diffusion in the Fe₂B layer.
- The Fe₂B iron boride nucleates after a specific incubation time.
- The boride layer grows because of the boron diffusion perpendicular to the specimen surface.
- Boron concentrations remain constant in the boride layer during the treatment.
- The influence of the alloying elements on the growth kinetics of the layer is not taken into account.

- The boride layer is thin compared to the sample thickness.
- A uniform temperature is assumed throughout the sample.
- A planar morphology is assumed for the phase interface.

The initial and boundary conditions for the diffusion problem are represented as:

$$t = 0, x > 0, \text{ with: } C_{Fe_2B} [x(t), t = 0] = C_0 \approx 0 \quad (1)$$

Boundary conditions:

$$C_{Fe_2B} [x(t=t_0^{Fe_2B}) = v_0, t = t_0^{Fe_2B}] = C_{up}^{Fe_2B} \quad (2)$$

(the upper boron concentration is kept constant) for $C_{ads}^B > 60 \cdot 10^3 \text{ mol m}^{-3}$:

$$C_{Fe_2B} [x(t=t) = v, t = t] = C_{low}^{Fe_2B} \quad (3)$$

(the upper boron concentration is kept constant) for $C_{ads}^B < 59.8 \cdot 10^3 \text{ mol m}^{-3}$

v_0 is a thin layer with a thickness of $\approx 5 \text{ nm}$ that formed during the nucleation stage,²⁰ thus $v_0 (\approx 0)$ is used when compared to the thickness of the Fe₂B layer (v). The mass-balance equation at the Fe₂B/substrate interface can be formulated with Equation (4) as follows:

$$\left(\frac{C_{up}^{Fe_2B} + C_{low}^{Fe_2B} - 2C_0}{2} \right) (A \cdot dv) = \quad (4)$$

$$= J_{Fe_2B} (x=v, t=t)(A \cdot dt) - J_{Fe} (x=v+dv, t=t)(A \cdot dt)$$

where $A(=1.1)$ is defined as the unit area and C_0 represents the boron concentration in the matrix. The fluxes J_{Fe_2B} and J_{Fe} are obtained from the Fick's first law as:

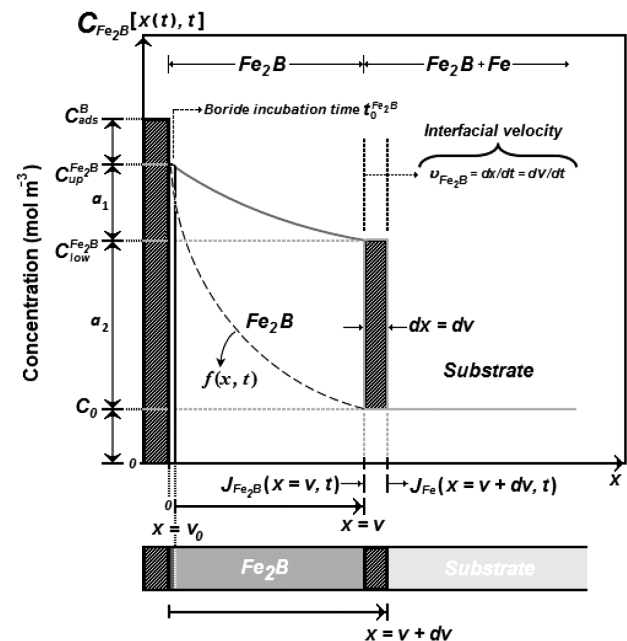


Figure 1: Schematic boron-concentration profile through the Fe₂B layer

Slika 1: Shematski prikaz profila koncentracije bora skozi Fe₂B-plast

$$\begin{aligned}
J_{\text{Fe}_2\text{B}} [x(t=t)=v, t=t] &= \\
&= - \left\{ \frac{D_{\text{Fe}_2\text{B}} \partial C_{\text{Fe}_2\text{B}} [x(t=t)=v, t=t]}{\partial x} \right\}_{x=v} \quad (5) \\
&\left(\frac{C_{\text{up}}^{\text{Fe}_2\text{B}} + C_{\text{low}}^{\text{Fe}_2\text{B}} - 2C_0}{2} \right) \varepsilon = \\
&= \sqrt{\frac{1}{\pi}} \left(\frac{C_{\text{up}}^{\text{Fe}_2\text{B}} - C_{\text{low}}^{\text{Fe}_2\text{B}}}{\text{erf}(\varepsilon)} \right) \exp(-\varepsilon^2) \quad (11)
\end{aligned}$$

and:

$$\begin{aligned}
J_{\text{Fe}} [x(t=t)=v+dv, t=t] &= \\
&= - \left\{ \frac{D_{\text{Fe}} \partial C_{\text{Fe}} [x(t=t)=v+dv, t=t]}{\partial x} \right\}_{x=v+dv} \quad (6)
\end{aligned}$$

The term J_{Fe} is zero since the boron solubility in the matrix is very low ($\approx 0 \text{ mol m}^{-3}$).³

Thus, Equation (4) can be written as:

$$\begin{aligned}
&\left(\frac{C_{\text{up}}^{\text{Fe}_2\text{B}} + C_{\text{low}}^{\text{Fe}_2\text{B}} - 2C_0}{2} \right) \frac{dx(t)}{dt} \Bigg|_{x(t)=v} = \\
&= -D_{\text{Fe}_2\text{B}} \frac{\partial C_{\text{Fe}_2\text{B}} [x(t=t), t=t]}{\partial x} \Bigg|_{x(t)=v} \quad (7)
\end{aligned}$$

The Fick's second law of diffusion relating to the change in the boron concentration through the Fe_2B layer with the time t and the distance $x(t)$ is given with Equation (8) :

$$\frac{\partial C_{\text{Fe}_2\text{B}} [x(t), t]}{\partial t} = D_{\text{Fe}_2\text{B}} \frac{\partial^2 C_{\text{Fe}_2\text{B}} [x(t), t]}{\partial x^2} \quad (8)$$

When applying the boundary conditions proposed in Equations (2) and (3), the solution of Equation (8) takes the following form:

$$C_{\text{Fe}_2\text{B}} [x(t), t] = C_{\text{up}}^{\text{Fe}_2\text{B}} + \frac{C_{\text{low}}^{\text{Fe}_2\text{B}} - C_{\text{up}}^{\text{Fe}_2\text{B}}}{\text{erf}\left(\frac{v}{2\sqrt{D_{\text{Fe}_2\text{B}}t}}\right)} \cdot \text{erf}\left(\frac{x}{2\sqrt{D_{\text{Fe}_2\text{B}}t}}\right) \quad (9)$$

By substituting the derivative of Equation (9) with respect to the distance $x(t)$ in Equation (7), Equation (10) is obtained:

$$\begin{aligned}
&\left(\frac{C_{\text{up}}^{\text{Fe}_2\text{B}} + C_{\text{low}}^{\text{Fe}_2\text{B}} - 2C_0}{2} \right) \frac{dv}{dt} = \\
&= \sqrt{\frac{D_{\text{Fe}_2\text{B}}}{\pi t}} \cdot \frac{(C_{\text{up}}^{\text{Fe}_2\text{B}} - C_{\text{low}}^{\text{Fe}_2\text{B}})}{\text{erf}\left(\frac{v}{2\sqrt{D_{\text{Fe}_2\text{B}}t}}\right)} \cdot \exp\left(-\frac{v^2}{4D_{\text{Fe}_2\text{B}}t}\right) \quad (10)
\end{aligned}$$

for $0 \leq x \leq v$.

Substituting the expression of the parabolic growth law ($v = 2\varepsilon\sqrt{D_{\text{Fe}_2\text{B}}t}$) in Equation (10), Equation (11) is deduced:

The normalized growth parameter (ε) for the Fe_2B /substrate interface can be estimated numerically using the Newton-Raphson method. It is assumed that expressions $C_{\text{up}}^{\text{Fe}_2\text{B}}$, $C_{\text{low}}^{\text{Fe}_2\text{B}}$ and C_0 do not depend significantly on the temperature (in the considered temperature range).¹⁸

A schematic representation of the square of the layer thickness against the linear time ($v^2 = 4\varepsilon^2 D_{\text{Fe}_2\text{B}} t = 4\varepsilon^2 D_{\text{Fe}_2\text{B}} [t_v + t_0^{\text{Fe}_2\text{B}}(T)]$) is depicted in **Figure 2**. $t_v (= t - t_0^{\text{Fe}_2\text{B}})$ is the effective growth time of the Fe_2B layer and t is the treatment time.

3 EXPERIMENTAL PROCEDURE

3.1 Boriding process

The AISI 4140 steel was used in this experimental study. It had a nominal chemical composition of 0.38–0.43 % C, 0.75–1.00 % Mn, 0.80–1.10 % Cr, 0.15–0.30 % Si, 0.040 % S, and 0.035 % P. Samples had a cubic shape with dimensions of 10 mm × 10 mm × 10 mm. Prior to the boriding process, the specimens were polished, ultrasonically cleaned in an alcohol solution and deionized water for 15 min at room temperature, dried and stored under clean-room conditions. The samples were packed along with a Durborid fresh powder mixture in a closed cylindrical case (AISI 304L). The used powder mixture had an average size of 30 μm . The powder-pack boriding process was carried out in a conventional furnace under a pure argon atmosphere in the temperature range of 1123–1273 K. Four treatment times (2, 4, 6 and 8 h) were selected for each temperature. After the completion of the boriding treatment, the container was removed from the furnace and slowly cooled to room temperature.

3.2 Microscopical observations of boride layers

The borided samples were cross-sectioned for metallographic examinations using a LECO VC-50 precision cutting machine. The cross-sectional morphology of the boride layers was observed with an Olympus GX51 light microscope in a clear field. **Figure 3** shows cross-sectional views of light images of the Fe_2B layers of the AISI 4140 steel formed at a temperature of 1223 K over different process durations.

The resultant microstructures of the Fe_2B layers appear to be very dense and homogenous, exhibiting saw-tooth morphologies. Since the growth of a saw-tooth boride layer is a controlled diffusion process with a highly anisotropic nature, higher temperatures and/or

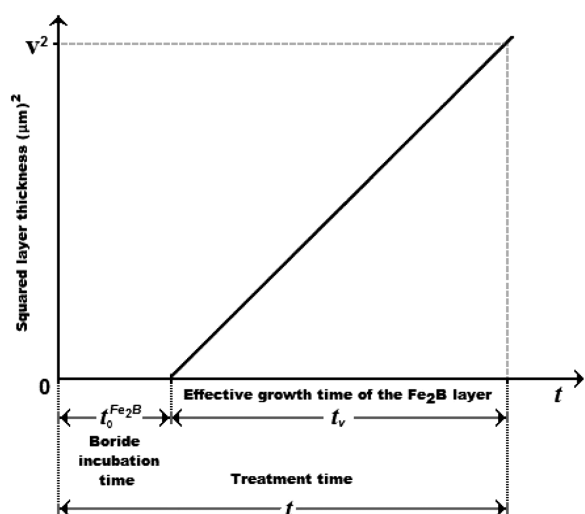


Figure 2: Schematic representation of the square of the layer thickness against the treatment time

Slika 2: Shematski prikaz kvadrata debeline plasti, odvisno od časa obdelave

longer times stimulated the Fe₂B crystals to make contact with the adjacent crystals and forced them to retain an acicular shape.²¹ It is seen that the thickness of the Fe₂B layer increased with an increase in the boriding time (Figure 3) because the boriding kinetics is influenced by the treatment time. For the kinetic study, the boride-layer thickness was automatically measured with the aid of the MSQ PLUS software. To ensure the reproducibility of the measured layer thicknesses, fifty measurements were collected in different sections of the samples of the borided AISI 4140 steel to estimate the Fe₂B layer thickness, defined as the average value of the long boride teeth.^{22–24} All the thickness measurements were taken from a fixed reference on the surface of the borided AISI 4140 steel, as illustrated in Figure 4.

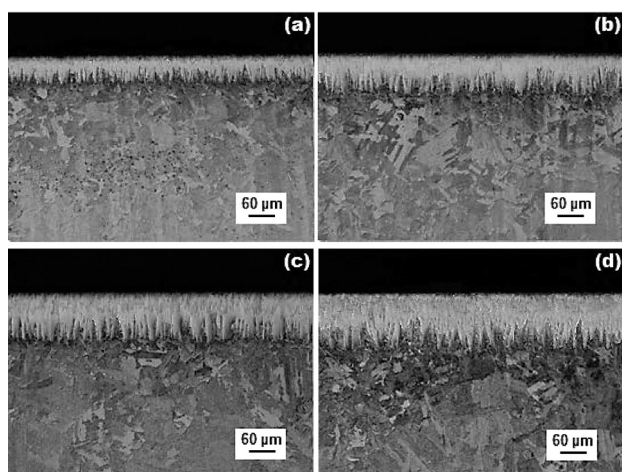


Figure 3: Light micrographs of the boride layers formed on the surface of AISI 4140 steel treated at 1223 K for variable times: a) 2 h, b) 4 h, c) 6 h and d) 8 h

Slika 3: Svetlobni posnetki boriranih plasti, nastalih na površini jekla AISI 4140 pri temperaturi 1223 K in različnem trajanju: a) 2 h, b) 4 h, c) 6 h in d) 8 h

The phases of the boride layers were investigated with X-ray diffraction (XRD) equipment (Equinox 2000) using Co-K_α radiation with a wavelength of 0.179 nm. The elemental distribution within the cross-section of a boride layer was determined with electron dispersive spectroscopy (EDS) equipment (JEOL JSM 6300 LV), from the surface.

4 RESULTS AND DISCUSSIONS

4.1 SEM observations and EDS analyses

A cross-sectional view of the SEM micrograph of the AISI 4140 steel borided at 1273 K for 6 h is shown in Figure 5a. The boride layer grown on the substrate has a saw-tooth morphology. The needles of Fe₂B, with different lengths, are visible on the SEM micrograph, penetrating into the substrate. This typical morphology is responsible for a good adhesion to the substrate. EDS results obtained with SEM are shown in Figures 5b and 5c. These results indicate the presence of two elements at the surface: Fe and Cr (Figure 5a). The results also show the possible dissolution of chromium in Fe₂B. In fact, the atomic radius of Cr (= 0.166 nm) is about the same and larger than that of Fe (= 0.155 nm), and it can then be expected that Cr dissolved in the Fe sublattice of Fe₂B. The obtained result in Figure 5c indicates the presence of the following elements: Fe, C, Cr, Si and Mn in the vicinity of the Fe₂B/substrate interface. It is seen that two elements (carbon and silicon) are not dissolved in Fe₂B, being displaced towards the substrate. Silicon and boron may form complex phases such as FeSi_{0.4}B_{0.6}, FeSiB and boron cementite (Fe₃B_{0.67}C_{0.33}).²⁵

4.2 X-ray diffraction analysis

Figure 6 displays the XRD pattern recorded on the surface of the AISI 4140 steel borided at a temperature of 1273 K for a treatment time of 8 h. The diffraction peaks relative to the Fe₂B phase are easily identified. Peaks with very small intensities are also observed for

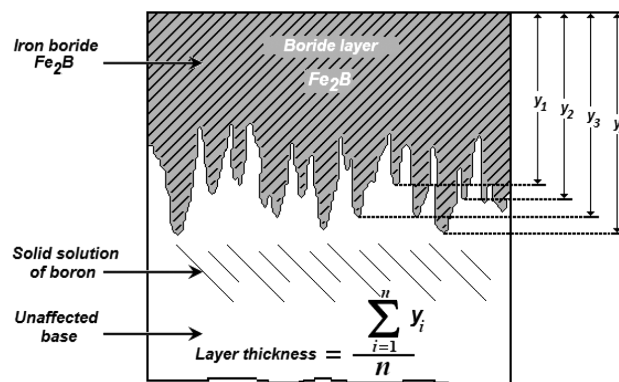


Figure 4: Schematic diagram illustrating the procedure for estimating the boride-layer thickness on the AISI 4140 steel

Slika 4: Shematski diagram, ki prikazuje postopek za ugotavljanje debeline borirane plasti na jeklu AISI 4140

the FeB phase but the Fe₂B phase is dominant with high-peak intensities. The CrB phase is also visible in the XRD pattern recorded at the surface of the borided AISI 4140 steel. In the experimental study about the boriding of the AISI 4140 steel in molten borax, boric acid and a ferro-silicon bath performed by Sen et al.²⁶, the XRD study showed the presence of FeB, Fe₂B and CrB at the surface of a sample borided at 1223 K for 6 h. In addition, Ulutan et al.²⁷ also identified, with an XRD analysis, the same phases at the surface of the AISI 4140 steel (at 1000 °C for 6 h) after the powder-pack boriding.

Crystals of the Fe₂B type orientate themselves with the z-axis perpendicular to the surface. Consequently, the peaks of the Fe₂B phase belonging to the crystallographic planes and having a deviation from zero of the *l* index, showed increased intensities in the X-ray diffraction spectra.²⁸

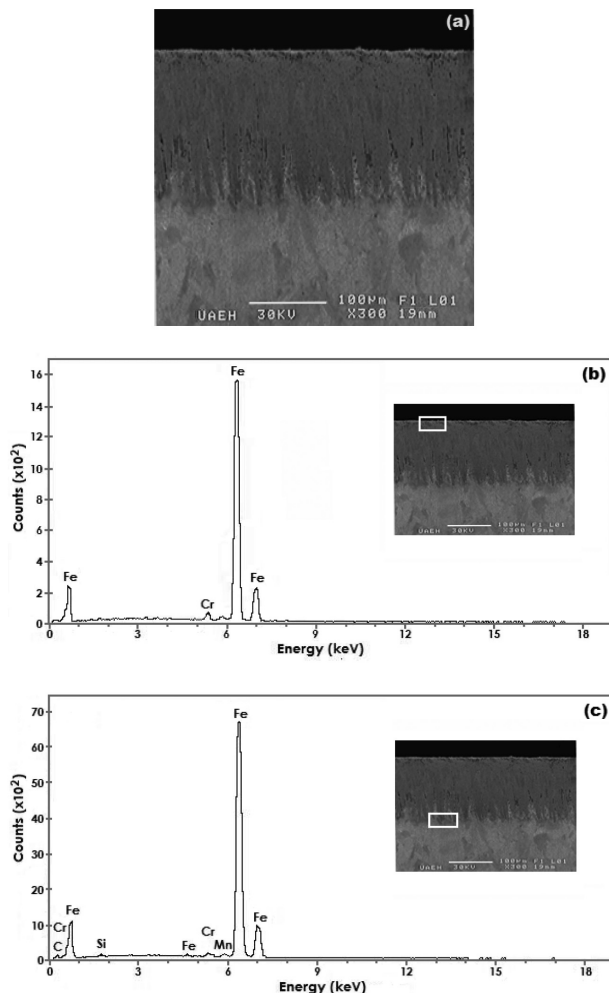


Figure 5: a) SEM micrograph of the cross-section of the AISI 4140 steel borided at 1273 K for 6 h, b) EDS spectrum of the surface of a borided sample and c) EDS spectrum of the interface of a borided sample

Slika 5: a) SEM-posnetek prereza boriranega jekla AISI 4140 po 6 h na 1273 K, b) EDS-spekter boriranega vzorca na površini in c) EDS-spekter boriranega vzorca na stiku z osnovo

The growth of boride layers is a controlled diffusion process with a highly anisotropic nature. In the case of the Fe₂B phase, the [001] crystallographic direction is the easiest path for the boron diffusion in Fe₂B because of the tendency of the boride crystals to grow along the direction of minimum resistance, perpendicular to the external surface. As the metal surface is covered, an increasing number of the Fe₂B crystals come in contact with the adjacent crystals, being forced to grow inside the metal and retaining the acicular shape.²¹ In the powder-pack boriding, the active boron is supplied by the powder mixture. To form a Fe₂B phase on any borided steel, a low boron potential is required as reported in the reference works^{4,29}, while a high amount of active boron in a powder mixture gives rise to a bilayer configuration consisting of FeB and Fe₂B.

4.3 Estimation of the boron activation energy

The growth kinetics of the Fe₂B layers formed on the AISI 4140 steel was used to estimate the boron diffusion coefficient through the Fe₂B layers by applying the suggested diffusion model. The ε parameter is then determined by solving the mass-balance equation for the Fe₂B/substrate interface (Equation (11)) using the Newton-Raphson method. **Table 1** lists the estimated value of boron diffusion coefficient in Fe₂B at each temperature along with the squared value of normalized growth parameter ε determined from Equation (11). **Figure 7** depicts the time dependence of the squared value of the Fe₂B layer thickness. The slopes of the straight lines in this figure provide the values of the growth constants ($= 4\varepsilon^2 D_{\text{Fe}_2\text{B}}$) for each boriding temperature. The values of the boron diffusion coefficients in the Fe₂B layers can be determined by knowing the value of the ε parameter. The boride incubation times for Fe₂B can also be deduced from the straight lines displayed in **Figure 7** by extrapolating them to the boride-layer thickness of zero.

To estimate the boron activation energy for the AISI 4140 steel, it is necessary to plot the natural logarithm of

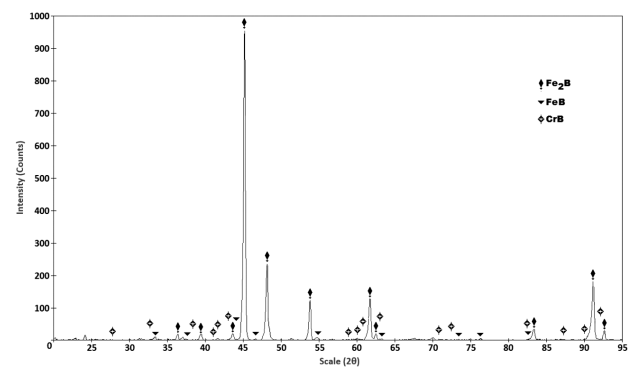


Figure 6: XRD pattern obtained at the surface of the borided AISI 4140 steel treated at 1273 K for 8 h

Slika 6: Rentgenogram, dobljen na površini boriranega jekla AISI 4140 po 8 h na 1273 K

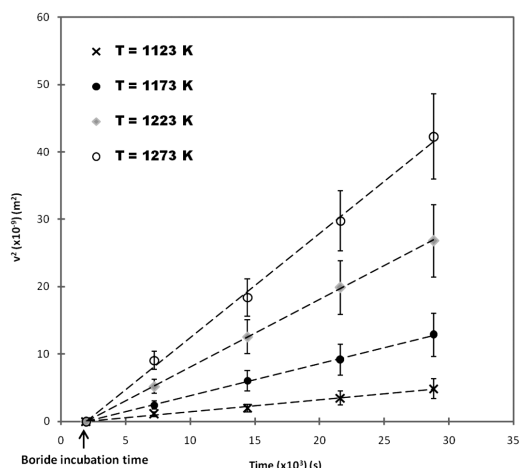


Figure 7: Evolution of the squared value of Fe₂B layer thickness as a function of boriding time

Slika 7: Razvoj vrednosti kvadrata debeline plasti Fe₂B v odvisnosti od časa boriranja

Table 1: Squared value of normalized growth parameter and boron diffusion coefficients for Fe₂B as a function of boriding temperature

Tabela 1: Kvadratna vrednost normaliziranih parametrov rasti in koeficientov difuzije bora v Fe₂B v odvisnosti od temperature boriranja

Temperature (K)	Type of layer	ε^2 (Dimensionless)	$4\varepsilon^2 D_{Fe_2B}$ ($\mu m^2 s^{-1}$)
1123	Fe ₂ B	1.7×10^{-3}	1.51×10^{-1}
1173			4.11×10^{-1}
1223			9.12×10^{-1}
1273			16.3×10^{-1}

the boron diffusion coefficient for Fe₂B versus the reciprocal temperature following the Arrhenius equation (Figure 8). A linear fitting was assumed to obtain the temperature dependence of the boron diffusion coefficient for Fe₂B with a correlation factor of 0.9935:

$$D_{Fe_2B} = 151 \times 10^{-2} \exp\left(\frac{-189.24 \text{ kJ mol}^{-1}}{RT}\right) \quad (12)$$

where $R = 8.3144621 \text{ J mol}^{-1} \text{ K}^{-1}$ and T is the absolute temperature in Kelvin.

Table 2 shows a comparison of the boron activation energies for some borided steels.^{26,30-32} The found value of the boron activation energy ($= 189.24 \text{ kJ mol}^{-1}$) for the AISI 4140 steel is slightly different from the value reported in²⁶ due to the boriding conditions (using the liquid-boriding method).

4.4 Validation of the diffusion model

The present model was validated by comparing the experimental value of the Fe₂B layer thickness with the predicted result at a temperature of 1253 K for a treatment time of 5 h using Equation (13):

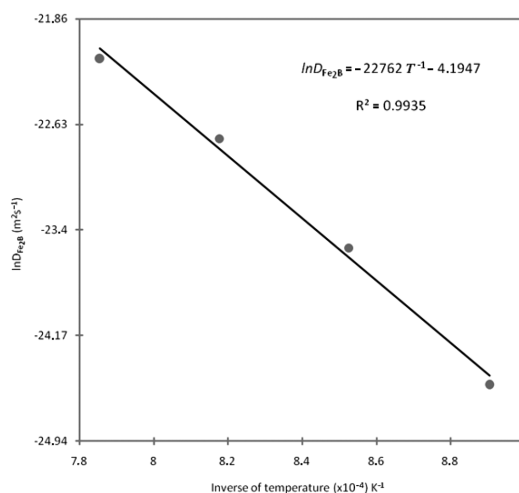


Figure 8: Temperature dependence of the boron diffusion coefficient for Fe₂B

Slika 8: Temperaturna odvisnost koeficienta difuzije v Fe₂B

Table 2: Comparison of the boron activation energies for some borided steels

Tabela 2: Primerjava aktivacijskih energij bora pri nekaterih boriranih jeklih

Material	Boron activation energy (kJ mol ⁻¹)	References
AISI 5140	223	30
AISI 4340	324	30
AISI 1040	118.8	31
AISI 51100	106.0	32
AISI 4140	215	26
AISI 4140	189.24	Present study

$$v = \frac{4}{\sqrt{\pi}} \left(\frac{C_{up}^{Fe_2B} - C_{low}^{Fe_2B}}{C_{up}^{Fe_2B} + C_{low}^{Fe_2B}} \right) \cdot \frac{\exp(-\varepsilon^2)}{\text{erf}(\varepsilon)} \sqrt{D_{Fe_2B} t} \quad (13)$$

Figure 9 shows the optical image of the boride layer formed at 1253 K after 5 h of treatment.

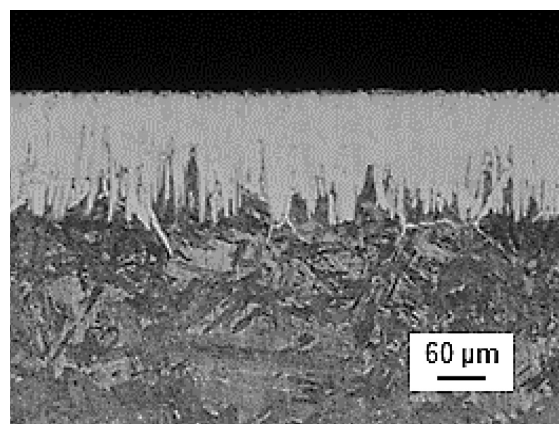


Figure 9: Light micrograph of the cross-section of the borided AISI 4140 treated at 1253 K for 5 h

Slika 9: Svetlobni posnetek prereza boriranega jekla AISI 4140 po 5 h na 1253 K

Table 3 gives a comparison between the experimental value of the Fe_2B layer thickness and the one predicted on the basis of Equation (13). A good agreement was obtained between the experimental value of the Fe_2B layer thickness and the predicted one for the AISI 4140 steel borided at 1253 K for 5 h.

Table 3: Predicted and estimated values of the Fe_2B layer thickness obtained at 1253 K for a treatment time of 5 h

Tabela 3: Predvidene in dobljene vrednosti za debelino plasti Fe_2B po 5 h na 1253 K

Temperature (K)	Type of layer	Boride-layer thickness (μm) estimated by Eq. (13)	Experimental boride-layer thickness (μm)
1253	Fe_2B	154.48	158.12 \pm 10.43

4.5 Future exploitation of the simulation results

This kinetic approach can be used as a tool to determine the Fe_2B layer thickness as a function of boriding parameters (time and temperature) for the AISI 4140 steel. Equation (13) predicts the Fe_2B layer thickness for any temperature and boriding time. An iso-thickness diagram was plotted as a function of the temperature and exposure time as shown in **Figure 10**.

The results of **Figure 10** can serve as a powerful tool to select the optimum value of the Fe_2B layer thickness in relation with the potential applications of the borided AISI 4140 steel at industrial scale.

As a rule, thin layers (e.g., 15–20 μm) are used to protect against adhesive wear (in the cases of chipless-shaping and metal-stamping dies and tools), whereas thick layers are recommended for combating abrasive wear (extrusion tooling for plastics with abrasive fillers and pressing tools for the ceramic industry). In the case of low-carbon steels and low-alloy steels, the optimum boride-layer thicknesses range from 50 μm to 250 μm . Finally, this model can be extended to predict the growth kinetics of a bilayer configuration ($\text{FeB} + \text{Fe}_2\text{B}$) grown on any boride steel.

5 CONCLUSIONS

The AISI 4140 steel was pack borided in the temperature range of 1123–1273 K over the treatment times varying from 2 h to 8 h. The Fe_2B layers were formed on the AISI 4140 steel substrate. A mathematical model was suggested to estimate the boron diffusion coefficients for the Fe_2B layers. The boron activation energy for the AISI 4140 steel was found to be 189.24 kJ mol⁻¹. This value was compared with the data reported in the literature.

The validity of the diffusion model was examined by comparing the experimental value of the Fe_2B layer thickness obtained at 1253 K after 5 h of treatment with that predicted by the model.

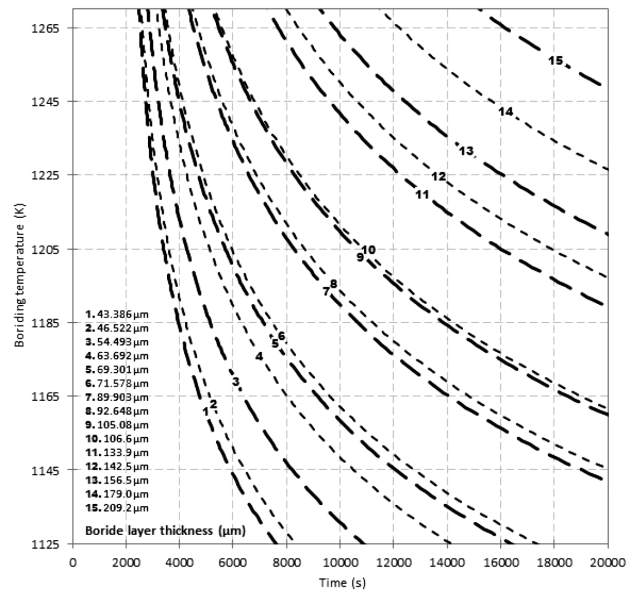


Figure 10: Iso-thickness diagram describing the evolution of Fe_2B layer as a function of boriding parameters

Slika 10: Diagram enakih debelin, ki opisuje nastanek Fe_2B -plasti v odvisnosti od parametrov boriranja

Finally, an iso-thickness diagram was proposed to be used as a tool to select the optimum boride layer thickness in relation with the industrial use of this steel grade.

NOMENCLATURE

v is the boride-layer thickness (m)

t_v is the effective growth time of the Fe_2B layer (s)

t is the treatment time (s)

$t_0^{\text{Fe}_2\text{B}}$ is the boride incubation time (s)

$C_{\text{up}}^{\text{Fe}_2\text{B}}$ represents the upper limit of the boron content in Fe_2B ($60 \cdot 10^3 \text{ mol m}^{-3}$)

$C_{\text{low}}^{\text{Fe}_2\text{B}}$ is the lower limit of the boron content in Fe_2B ($59.8 \cdot 10^3 \text{ mol m}^{-3}$)

$C_{\text{ads}}^{\text{B}}$ is the adsorbed boron concentration in the boride layer (mol m^{-3})

$a_1 = C_{\text{up}}^{\text{Fe}_2\text{B}} - C_{\text{low}}^{\text{Fe}_2\text{B}}$ defines the homogeneity range of the Fe_2B layer (mol m^{-3})

$a_2 = C_{\text{low}}^{\text{Fe}_2\text{B}} - C_0$ is the miscibility gap (mol m^{-3})

C_0 is the terminal solubility of the interstitial solute ($\approx 0 \text{ mol m}^{-3}$)

$C_{\text{Fe}_2\text{B}} [x(t)]$ is the boron concentration profile in the Fe_2B layer (mol m^{-3})

v_0 indicates the initial Fe_2B layer (m)

ε is the normalized growth parameter for the Fe_2B /substrate interface (it has no physical dimensions)

$D_{\text{Fe}_2\text{B}}$ denotes the diffusion coefficient of boron in the Fe_2B phase ($\text{m}^2 \text{ s}^{-1}$)

$J_i [x(t)]$, (with $i = \text{Fe}_2\text{B}$ and Fe) are the fluxes of boron atoms at the Fe_2B /substrate interface boundary ($\text{mol m}^{-2} \text{ s}^{-1}$)

Acknowledgements

The work described in this paper was supported by a grant of CONACyT and PROMEP, México. Also, the authors wish to thank Ing. Martín Ortiz Granillo, the Director of Escuela Superior de Ciudad Sahagún which is part of Universidad Autónoma del Estado de Hidalgo, México, for providing all the facilities necessary to accomplish this research work.

6 REFERENCES

- ¹ A. K. Sinha, Boriding (Boronizing) of Steels, ASM Handbook, vol. 4, ASM International, 1991, 437-447
- ² C. Meric, S. Sahin, S. S. Yilmaz, Mater. Res. Bull., 35 (2000) 13, 2165–2172, doi:10.1016/S0025-5408(00)00427-X
- ³ H. Okamoto, J. Phase Equilib. Diff., 25 (2004) 3, 297–298, doi:10.1007/s11669-004-0128-3
- ⁴ J. Vipin, G. Sundararajan, Surf. Coat. Technol., 149 (2002), 21–26, doi:10.1016/S0257-8972(01)01385-8
- ⁵ A. Pertek, M. Kulka, Appl. Surf. Sci., 202 (2002), 252–260, doi:10.1016/S0169-4332(02)00940-6
- ⁶ I. Campos, J. Oseguera, U. Figueroa, J. A. Garcia, O. Bautista, G. Keleminis, Mater. Sci. Eng. A, 352 (2003) 1–2, 261–265, doi:10.1016/S0921-5093(02)00910-3
- ⁷ M. Keddám, Appl. Surf. Sci., 236 (2004) 1, 451–455, doi:10.1016/j.apsusc.2004.05.141
- ⁸ R. D. Ramdan, T. Takaki, Y. Tomita, Mater. Trans., 49 (2008) 11, 2625–2631
- ⁹ D. S. Kukharev, S. P. Fizenko, S. I. Shabunya, J. Eng. Phys. Therm., 69 (1996) 2, 187–193, doi:10.1007/BF02607937
- ¹⁰ M. Keddám, M. Ortiz-Domínguez, I. Campos-Silva, J. Martínez-Trinidad, Appl. Surf. Sci., 256 (2010) 10, 3128–3132, doi:10.1016/j.apsusc.2009.11.085
- ¹¹ I. Campos-Silva, M. Ortiz-Domínguez, H. Cimenoglu, R. Escobar-Galindo, M. Keddám, M. Elías-Espinosa, N. López-Perrusquia, Surf. Eng., 27 (2011) 3, 189–195, doi:10.1179/026708410X12550773057820
- ¹² M. Ortiz-Domínguez, E. Hernandez-Sanchez, J. Martínez-Trinidad, M. Keddám, I. Campos-Silva, Kovove Mater., 48 (2010) 5, 285–290
- ¹³ I. Campos-Silva, N. López-Perrusquia, M. Ortiz-Domínguez, U. Figueroa-López, O. A. Gómez-Vargas, A. Meneses-Amador, G. Rodríguez-Castro, Kovove Mater., 47 (2009) 2, 75–81
- ¹⁴ M. Keddám, R. Chegroune, Appl. Surf. Sci., 256 (2010) 16, 5025–5030, doi:10.1016/j.apsusc.2010.03.048
- ¹⁵ M. Ortiz-Domínguez, M. Keddám, M. Elías-Espinosa, O. Damián-Mejía, M. A. Flores-Rentería, A. Arenas-Flores, J. Hernández-Ávila, Surf. Eng., 30 (2014), 490–497, doi:10.1179/1743294414Y.0000000273
- ¹⁶ M. Elías-Espinosa, M. Ortiz-Domínguez, M. Keddám, M. A. Flores-Rentería, O. Damián-Mejía, J. Zuno-Silva, J. Hernández-Ávila, E. Cardoso-Legorreta, A. Arenas-Flores, J. Mater. Eng. Perform., 23 (2014), 2943–2952, doi:10.1007/s11665-014-1052-2
- ¹⁷ M. Kulka, N. Makuch, A. Pertek, L. Maldzinski, J. Solid State Chem., 199 (2013), 196–203, doi:10.1016/j.jssc.2012.12.029
- ¹⁸ C. M. Brakman, A. W. J. Gommers, E. J. Mittemeijer, J. Mater. Res., 4 (1989), 1354–1370, doi:10.1557/JMR.1989.1354
- ¹⁹ L. G. Yu, X. J. Chen, K. A. Khor, G. Sundararajan, Acta Mater., 53 (2005), 2361–2368, doi:10.1016/j.actamat.2005.01.043
- ²⁰ V. I. Dybkov, Reaction Diffusion and Solid State Chemical Kinetics, Trans Tech Publications, Switzerland-UK-USA 2010, 7
- ²¹ G. Palombarini, M. Carbucicchio, J. Mater. Sci. Lett., 6 (1987), 415–416, doi:10.1007/BF01756781
- ²² I. Campos-Silva, D. Bravo-Bárceñas, A. Meneses-Amador, M. Ortiz-Domínguez, H. Cimenoglu, U. Figueroa-López, J. Andraca-Adame, Surf. Coat. Technol., 237 (2013), 402–414, doi:10.1016/j.surfcoat.2013.06.083
- ²³ H. Kunst, O. Schaaber, Härtereitech. Mitt., 22 (1967), 275
- ²⁴ I. Campos-Silva, M. Ortiz-Domínguez, O. Bravo-Bárceñas, M. A. Doñu-Ruiz, D. Bravo-Bárceñas, C. Tapia-Quintero, M. Y. Jiménez-Reyes, Surf. Coat. Technol., 205 (2010), 403–412, doi:10.1016/j.surfcoat.2010.06.068
- ²⁵ I. S. Dukarevich, M. V. Mozharov, A. S. Shigarev, Metallovedenie Termicheskaya i Obrabotka Metallov, 2 (1973), 64–66, doi:10.1007/BF00679753
- ²⁶ S. Sen, U. Sen, C. Bindal, Vacuum, 77 (2005), 195–202, doi:10.1016/j.vacuum.2004.09.005
- ²⁷ M. Ulutan, M. M. Yildirim, O. N. Celik, S. Buytoz, Tribol. Lett., 38 (2010), 231–239, doi:10.1007/s11249-010-9597-1
- ²⁸ C. Badini, D. Mazza, J. Mater. Sci. Lett., 23 (1988), 661–665
- ²⁹ C. Bindal, A. H. Ucisik, Surf. Coat. Technol., 122 (1999), 208–213, doi:10.1016/S0257-8972(99)00294-7
- ³⁰ S. Sen, U. Sen, C. Bindal, Surf. Coat. Technol., 191 (2005) 2–3, 274–285, doi:10.1016/j.surfcoat.2004.03.040
- ³¹ O. N. Celik, N. Aydinbeyli, H. Gasan, Prakt. Metallogr., 45 (2008) 7, 334–347, doi:10.3139/147.100390
- ³² M. Ipek, G. Celebi Efe, I. Ozbek, S. Zeytin, C. Bindal, J. Mater. Eng. Perform., 21 (2012) 5, 733–738, doi:10.1007/s11665-012-0192-5